NURETH14-057

COUNTER-CURRENT FLOW LIMITATION AT THE JUNCTION BETWEEN THE SURGE LINE AND THE PRESSURIZER OF A PWR

T. Futatsugi¹, T. Nariai¹, K. Hayashi¹, A. Tomiyama¹, C. Yanagi², and M. Murase²

Graduate School of Engineering, Kobe University, Japan

Institute of Nuclear Safety System, Inc.

futatsugi@cfrg.scitec.kobe-u.ac.jp, hayashi@mech.kobe-u.ac.jp, yanagi.chihiro@inss.co.jp, nariai@cfrg.scitec.kobe-u.ac.jp tomiyama@mech.kobe-u.ac.jp murase@inss.co.jp

Abstract

An experimental study on counter-current flow limitation (CCFL) in vertical pipes is carried out to understand CCFL in the surge line in a PWR. Several upper tanks corresponding to the pressurizer and a lower tank are used to investigate effects of tank geometry and water levels in the tanks on CCFL characteristics. The experimental data clearly show that CCFL depends on the tank geometry and the water level, and therefore, these factors must be taken into account when modelling characteristics of CCFL in vertical pipes.

Keywords: PWR, Surge line, Counter-current flow, CCFL, Vertical pipe.

1. Introduction

During a PWR plant outage for maintenance and refueling, the reactor coolant is cooled by a residual heat removal (RHR) system. For a certain period, the reactor coolant level is kept around the primary loop center in order to carry out operations like aeration, attachment or detachment of the steam generator (SG) nozzle dam. This operation mode is called mid-loop operation. If a failure of the RHR system occurs during the mid-loop operation, there is a possibility of boiling of the reactor coolant. One of the effective methods to cool the reactor core in this event is reflux cooling by the SG. During the reflux condensation, steam generated in the reactor core and water condensed in a pressurizer due to heat transfer to its vessel wall may form a counter-current flow in a surge line connecting the hot leg and the pressurizer. Water levels in the reactor core and in the pressurizer depend on the counter-current flow behavior in the surge line, which consists of a vertical pipe and an inclined pipe with several elbows.

In our previous study [1], counter-current flow limitation (CCFL) in a scale-down model of a PWR surge line was investigated by measuring the relationship between the water and gas flow rates in the surge line. The relationship is referred to as CCFL characteristics. The CCFL takes place at three locations in the experiments, i.e., at the junction between the vertical pipe and the bottom of the pressurizer, in the inclined pipe and at the junction between the inclined pipe and the hot leg. Hereafter they will be referred to as CCFL-U, CCFL-S and CCFL-L, respectively.

The CCFL characteristics strongly depend on the location of CCFL. The experiments imply that the CCFL at the junction between the vertical pipe and the bottom of the pressurizer plays an important role in the actual surge line under the reflux cooling.

Many studies on CCFL in vertical pipes have been carried out [2-10] using the experimental apparatus consisting of a vertical pipe, an upper tank and a lower tank. Although a number of experimental data of CCFL for various diameters, lengths and end geometries of vertical pipes have been obtained [8-10], modeling of CCFL in vertical pipes is insufficient because of a large scatter in the data obtained for the different experiments. This scatter implies that the upper and lower tank geometries may have non-negligible influence on CCFL. Little has, however, been studied on the effect of tank geometry.

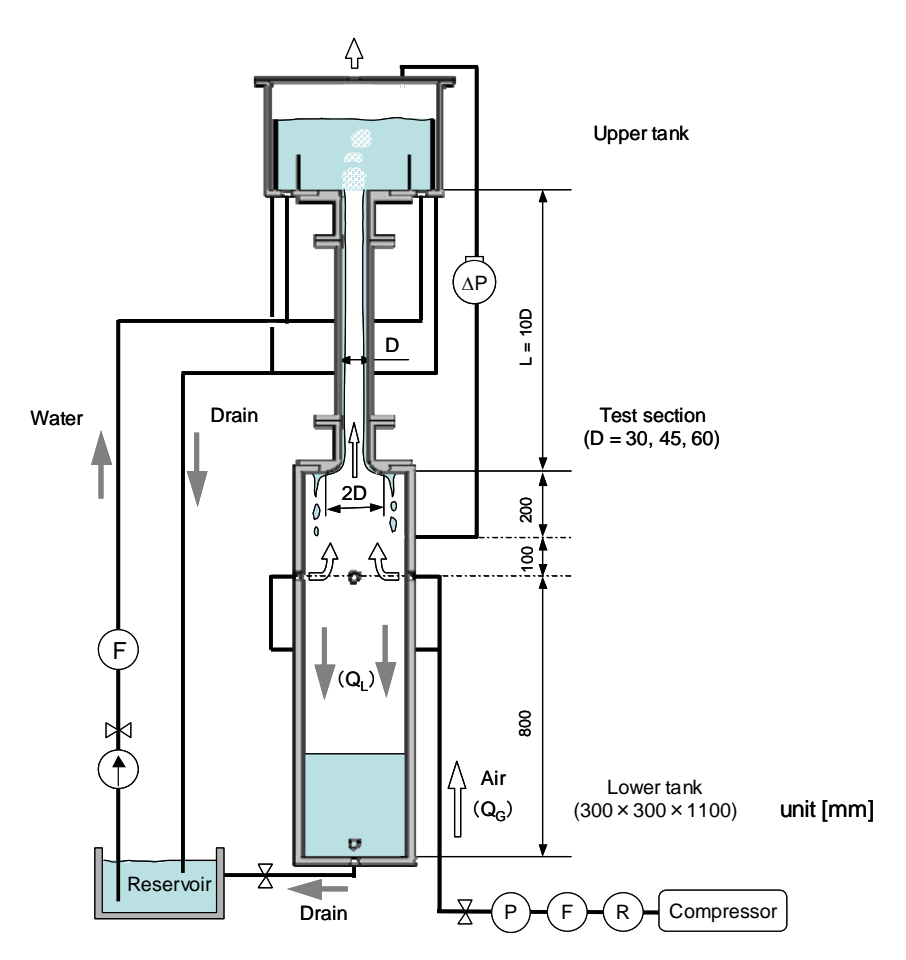
In the present study, the effects of upper tank geometry on CCFL characteristics were investigated by using a rectangular tank and a cylindrical tank. The flow rate of water entering into a lower tank was measured to obtain the CCFL characteristics. Flow patterns in the upper tanks were observed by using a high-speed video camera and the pressure difference between the upper and lower tanks was measured to understand relations between CCFL characteristics and flow patterns in the tanks. Furthermore effects of water levels in the cylindrical upper tank and the lower tank on CCFL characteristics were investigated.

2. Experimental

2.1 Experimental setup

Figure 1 shows the experimental setup. It consists of the upper tank which corresponds to the bottom part of the pressurizer, the vertical pipe corresponding to a part of the surge line, the lower tank, the air supply system and the water supply system. The pipe and tanks are made of transparent acrylic resin for observation. The diameters of vertical pipes are 30, 45 and 60 mm. Air was supplied from the oil-free compressor (SRL-11P6AI, Hitachi Ltd.), and flowed into the lower tank from four inlets through the regulator (R600-20, CKD) and the flowmeter (FLT, Flowcell, Ltd.). Tap water was supplied from the magnet pump (MX-F400, Iwaki, Ltd.) and flowed into the upper tank through the flowmeter (FLT-N, Flowcell, Ltd.). Experiments were carried out at room temperature and atmospheric pressure. The geometry of the junction between the upper tank and the vertical pipe and that of the junction between the lower tank and the vertical pipe are right angle and bell-mouth, respectively.

Three types of upper tanks, which we refer to as the rectangular tank, cylindrical tank (a) and cylindrical tank (b), are shown in Figures 2 (i), (ii) and (iii), respectively. The cylindrical tank (a) and the rectangular tank were used to investigate the effects of upper tank geometry on CCFL characteristics. Water levels in the upper tanks were kept constant by overflowing the supplied water. The effects of water level were investigated by using the cylindrical tank (b). The ratio of its diameter to the pipe diameter was determined so as to be analogous to the actual pressurizer. It has drain holes on its wall at various elevations. The drain holes used in each experiment were changed to test various water levels in the upper tank.



 $P: Pressure\ gage,\ F: Flow\ meter,\ R: Regulator,\ \Delta P: Differential\ pressure\ transducer$

Figure 1 Experimental setup

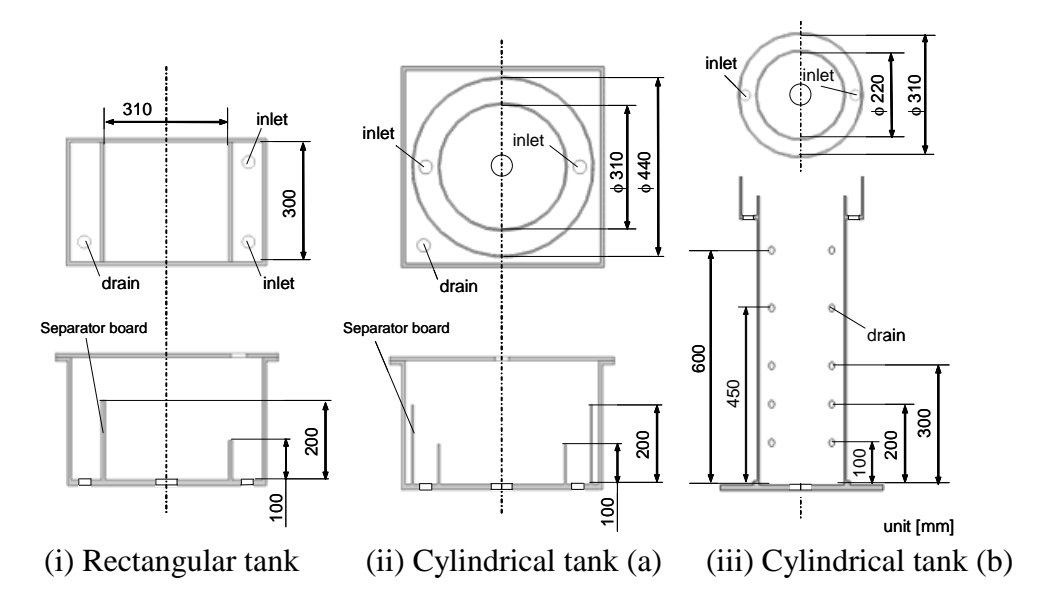


Figure 2 Upper tanks

2.2 Experimental method

2.2.1 CCFL characteristics

CCFL characteristics were investigated by measuring the flow rate, Q_L , of water entering into the lower tank at constant gas flow rates, Q_G . The Q_L was calculated from the rise speed of water level in the lower tank. The ranges of the liquid and gas volume fluxes, J_L and J_G , tested were $0 \le J_L \le 0.118$ m/s and $2.40 \le J_G \le 16.4$ m/s, respectively, where J_L and J_G are defined by

$$J_k = \frac{Q_k}{A} \qquad (k = L, G) \tag{1}$$

Here A is the cross-sectional area of the vertical pipe and the subscripts L and G denote the liquid and gas phases, respectively. The uncertainties in measured J_L and J_G estimated at 95 % confidence were \pm 3.0 % and \pm 2.5 %, respectively.

2.2.2 Pressure difference

The pressure difference ΔP (= P_{Lower} - P_{Upper} , where P_{Lower} and P_{Upper} are the pressures in the lower and upper tanks, respectively) was measured using a differential pressure transducer (DP45, Valydine, Ltd. natural frequency > 600 Hz). It was connected between the top of the upper tank and the side wall of the lower tank as shown in Figure 1. The sampling rate was 1.0 kHz and the measurement time was 30 seconds. The uncertainty in measured ΔP was less than 0.5 % of the full scale (6 kPa). Flows in the upper tank were observed by using a high-speed video camera (Dantec Dynamics, Nano sence Mk3) to understand the relation between ΔP and the flow behavior in the upper tank. The frame rate was 100 fps and the recording time was 30 s.

3. Results and discussion

3.1 Effects of upper tank geometry

Flow visualization with the high-speed video camera showed that the CCFL with the rectangular tank occurred only at the junction between the vertical pipe and the upper tank (CCFL-U) under all the test conditions. The CCFL characteristics measured using the rectangular tank are plotted in Figure 3 (i), where J_L^* and J_G^* are the Wallis parameters [11] defined by

$$J_{k}^{*} = J_{k} \left[\frac{\rho_{k}}{gD(\rho_{L} - \rho_{G})} \right]^{1/2} \qquad (k = L, G)$$
 (2)

where ρ is the density, g the acceleration of gravity and D the pipe diameter. At constant J_G^* , J_L^* becomes smaller with increasing D, i.e., the flow limitation becomes stronger. Figure 3 (ii) shows the CCFL characteristics for the cylindrical tank (a). The CCFL occurs only at the junction at low J_G^* , whereas some water penetrating into the vertical pipe intermittently flowed back into the

upper tank at high J_G^* and $D \le 45$ mm, i.e., the CCFL occurs not only at the junction but also inside the pipe (CCFL-P). The CCFL characteristics clearly depend on the pipe diameter and the location where CCFL takes place.

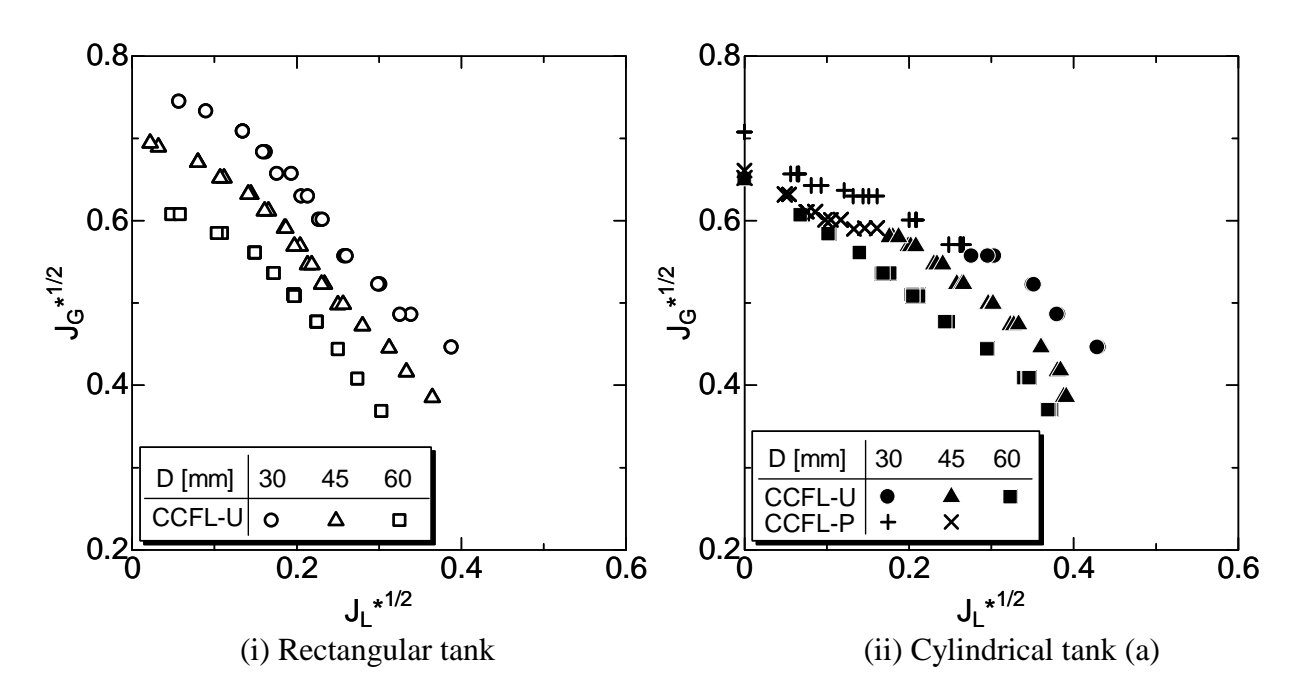


Figure 3 CCFL characteristics for rectangular and cylindrical tanks on ${J_G}^{*^{1/2}} - {J_L}^{*^{1/2}}$ plane

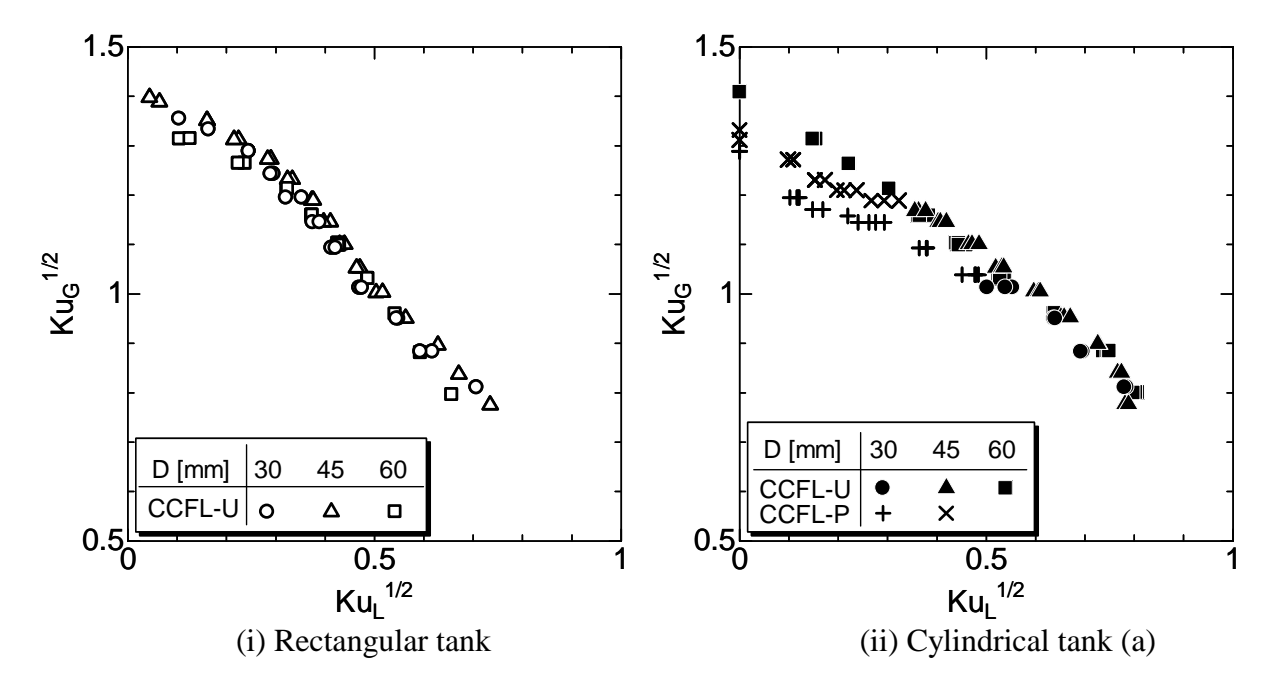


Figure 4 CCFL characteristics for rectangular and cylindrical tanks on $Ku_G*^{1/2}$ – $Ku_L*^{1/2}$ plane

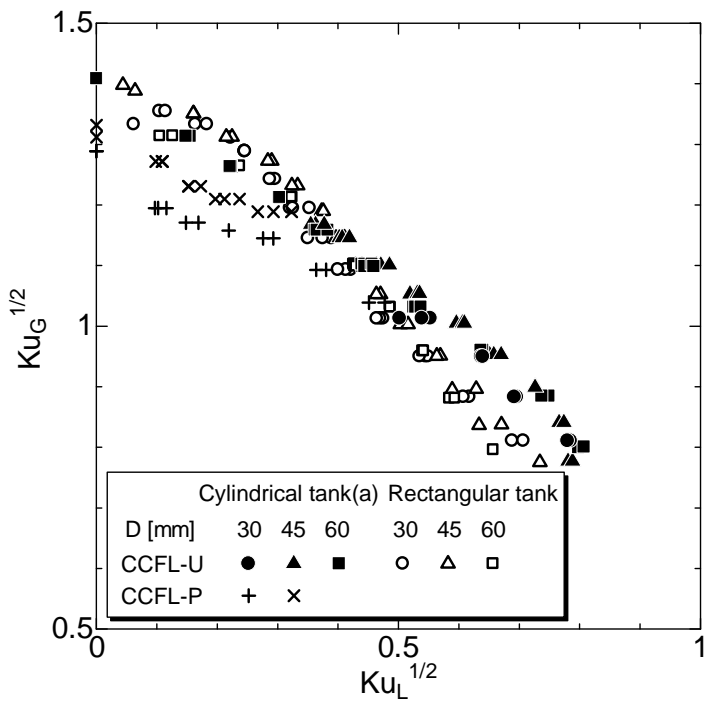


Figure 5 Effects of upper tank geometry on CCFL characteristics

The CCFL characteristics are re-plotted on the $Ku_L^{1/2} - Ku_G^{1/2}$ plane as shown in Figure 4, where Ku_L and Ku_G are the Kutateladze numbers [12] for the liquid and gas phases defined by

$$Ku_k = J_k \left[\frac{\rho_k^2}{g \,\sigma(\rho_L - \rho_G)} \right]^{1/4} \qquad (k = L, G)$$
(3)

where σ is the surface tension. The CCFL characteristics for different pipe diameters are well correlated with the Kutateladze numbers both for the rectangular and cylindrical tanks when the CCFL occurs only at the junction. The CCFL characteristics for the two tanks are compared in Figure 5. The flow limitation with the cylindrical tank (a) is stronger than that with the rectangular tank at high Ku_G because of the CCFL occurrence inside the pipe. On the other hand, at low Ku_G , the CCFL with the rectangular tank is stronger. This will be discussed later based on the observation of bubble motions in the upper tanks.

Figure 6 shows the pressure differences, ΔP , for the cylindrical and rectangular tanks and their power spectrums obtained by the fast Fourier transform analysis. The pressure fluctuations for the cylindrical tank (a) mainly consist of waves in the range of 5 - 7 Hz. On the other hand, those for the rectangular tank consist of single peaks at 3 Hz and broad peaks in the range of 5 - 10 Hz. Figure 7 shows a typical bubble generation process in the cylindrical tank (a) and ΔP at $J_G = 4.9$ m/s and D = 45 mm. There is no bubble at the junction at t = 0.13 s. The ΔP increases as a bubble starts to be generated at the junction until t = 0.18 s. The ΔP then decreases as the bubble grows for t = 0.18 s - 0.23 s. The bubble is released from the junction at t = 0.28 s, and then, the next bubble starts to be generated at 0.33 s. The period and the frequency of this process are about 0.20 s and 5 Hz, which corresponds to the peak frequency.

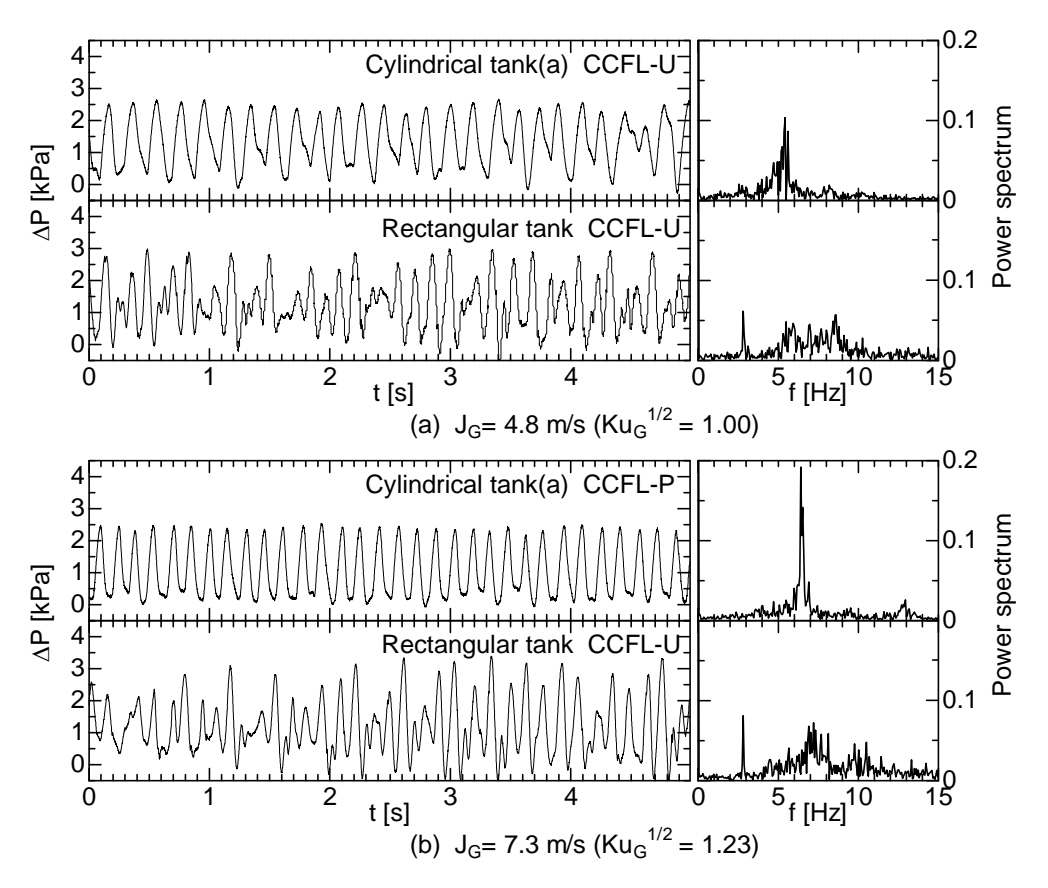


Figure 6 Pressure difference ΔP between upper and lower tanks (D = 45 mm)

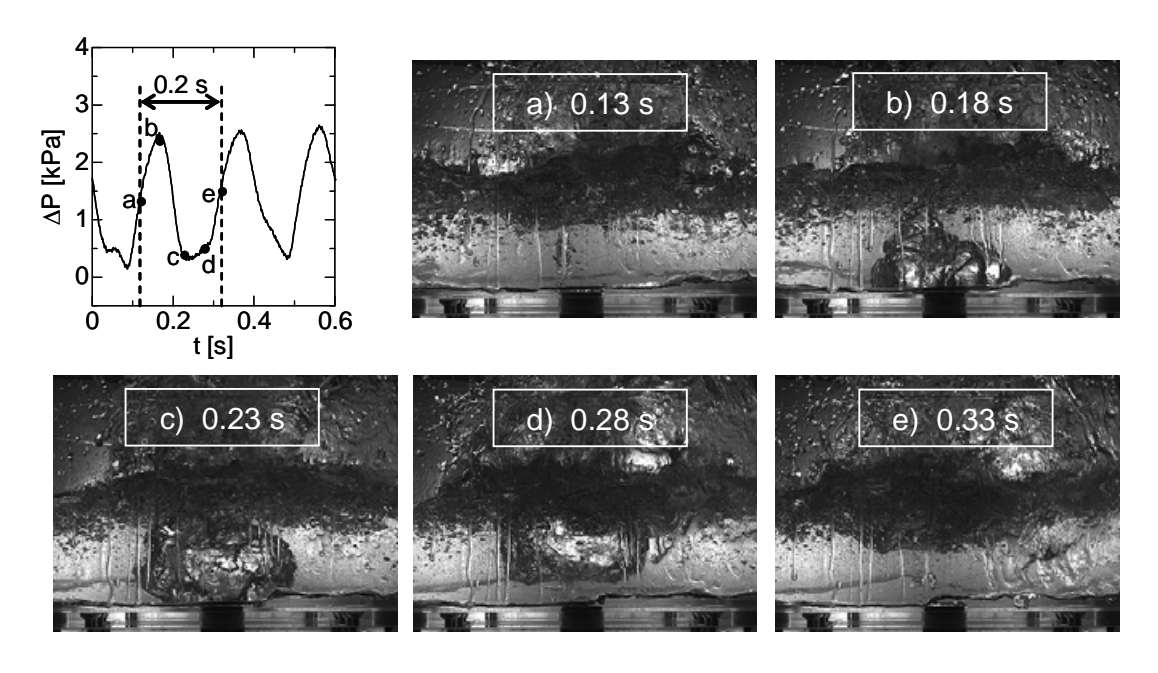


Figure 7 Bubble generation process in the cylindrical tank (a) $(J_G = 4.9 \text{ m/s}, J_G*^{1/2} = 0.50, Ku_G^{1/2} = 1.0 \text{ and } D = 45 \text{ mm})$

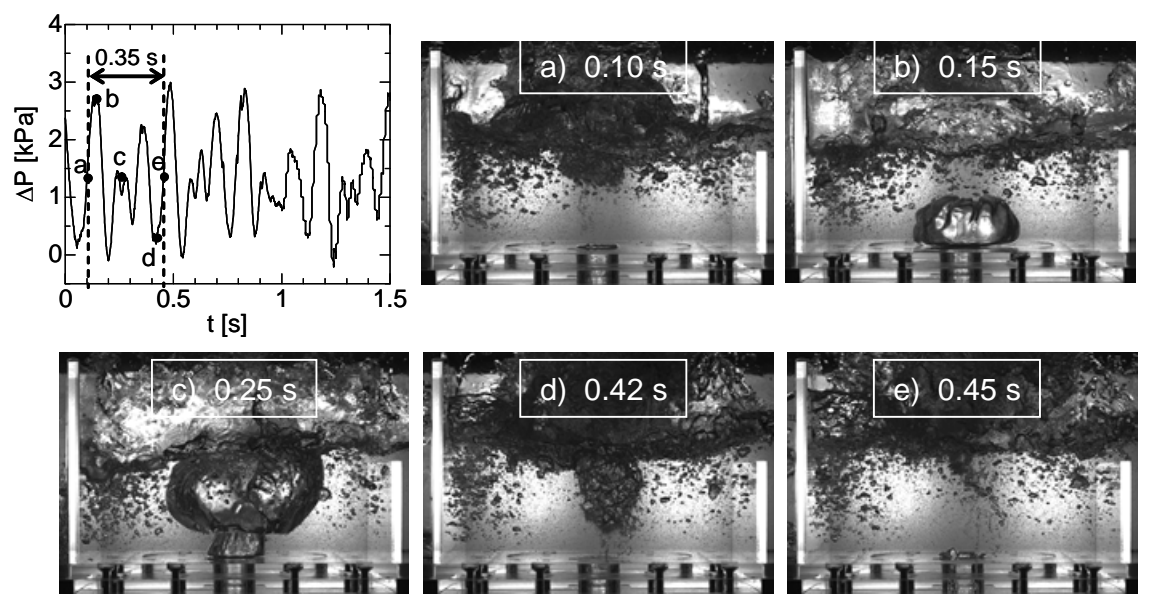


Figure 8 Bubble generation process in the rectangular tank $(J_G = 4.9 \text{ m/s}, J_G^{*^{1/2}} = 0.50, Ku_G^{1/2} = 1.0 \text{ and } D = 45 \text{ mm})$

A bubble generation process in the rectangular tank at $J_G = 4.9$ m/s and D = 45 mm is shown in Figure 8. The ΔP increases as the bubble grows at the junction for t = 0.10 - 0.15 s. For t > 0.15 s, a trailing bubble is formed behind the leading bubble. The fluctuation of ΔP for 0.15 < t < 0.42 s must be due to these trailing bubbles. The next leading bubble starts to grow at t = 0.45 s. The period of the generation of leading bubbles is 0.35 s. The single peak at 3 Hz and the broad peak in the range of 5 - 10 Hz in Figure 5, therefore, correspond to the leading-bubble generation cycle and the fluctuation due to the trailing bubbles, respectively. The first mode sloshing shown in Figure 9 was observed only for the rectangular tank. The free surface in the tank took the maximum inclination at t = 0 s as shown in Figure 9 (a). Then the water moved to the left side, and the bubble was detached from the junction due to water movement in the horizontal direction (Figure 9 (b)). Two leading bubbles were released during one period of the sloshing (Figures 9 (a) – (e)). The natural frequency of the first mode sloshing in a two dimensional rectangular tank is given by [13]

$$f = \frac{\sqrt{gk \tanh kH}}{2\pi} \qquad (k = \pi / L) \tag{4}$$

where H is the height of the free surface and L the width of the tank. According to Eq. (4), the frequency for the rectangular tank used is 1.53 Hz, which is about half of the bubble release frequency. The bubble release frequency is, therefore, strongly governed by the sloshing in the tank.

Figure 10 shows images of flows in the rectangular tank and the pipe. Water lump penetrated into the pipe when a bubble detached. The CCFL is therefore mitigated when the bubble release frequency is high. This might be the main reason why the CCFL with the rectangular tank is stronger than that with the cylindrical tank (a) at low Ku_G as shown in Figure 5.

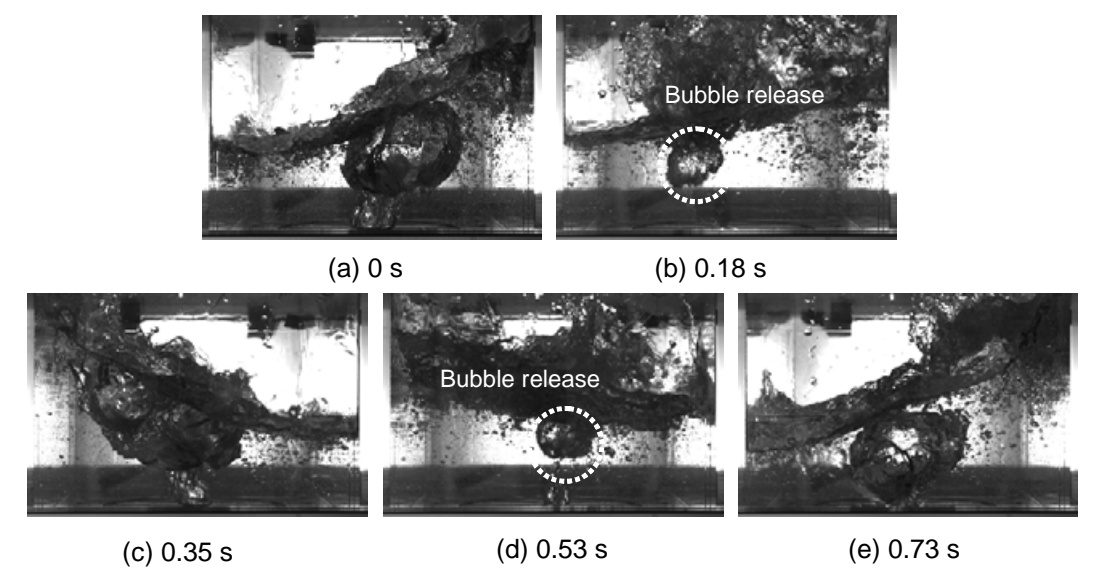


Figure 9 First mode sloshing in the rectangular tank $(J_G = 7.7 \text{ m/s}, J_G^{*^{1/2}} = 0.70, Ku_G^{1/2} = 1.3 \text{ and } D = 30 \text{ mm})$

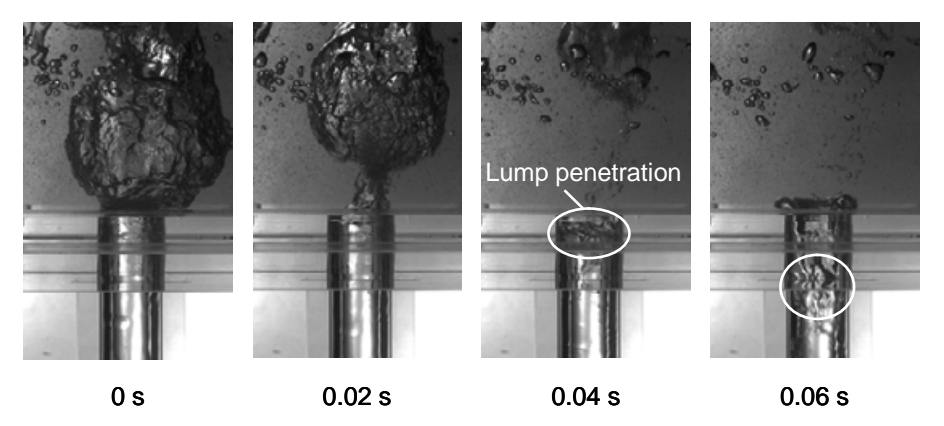


Figure 10 Relation between bubble release and water penetration $(J_G = 5.8 \text{ m/s}, J_G^{*1/2} = 0.60, Ku_G^{1/2} = 1.1 \text{ and } D = 30 \text{ mm})$

3.2 Effects of water level in tank

The CCFL characteristics measured using the cylindrical tank (b) shown in Figure 2 (iii) are discussed in this section. Various water levels in the upper and the lower tanks were tested. The water level in the lower tank was kept constant throughout the experiments by manually controlling the drain cock opening. In this case, Q_L was calculated from the amount of drain water. Figure 11 shows the CCFL characteristics for various water levels in the upper tank at constant water levels in the lower tank, where V_{Lower} is the lower tank volume occupied by the air and h the elevation of the drain holes in the upper tank. The CCFL becomes stronger as h decreases at $V_{Lower} = 0.039$ m³. The difference in the CCFL characteristics is, however, not so significant. On the other hand, the CCFL characteristics strongly depend on h at $V_{Lower} = 0.092$ m³. Effects of V_{Lower} are shown in Figure 12. The CCFL characteristics do not depend on V_{Lower} at h = 200 mm, whereas the influence of V_{Lower} is significant at h = 600 mm, i.e., the increase in V_{Lower} makes the CCFL stronger.

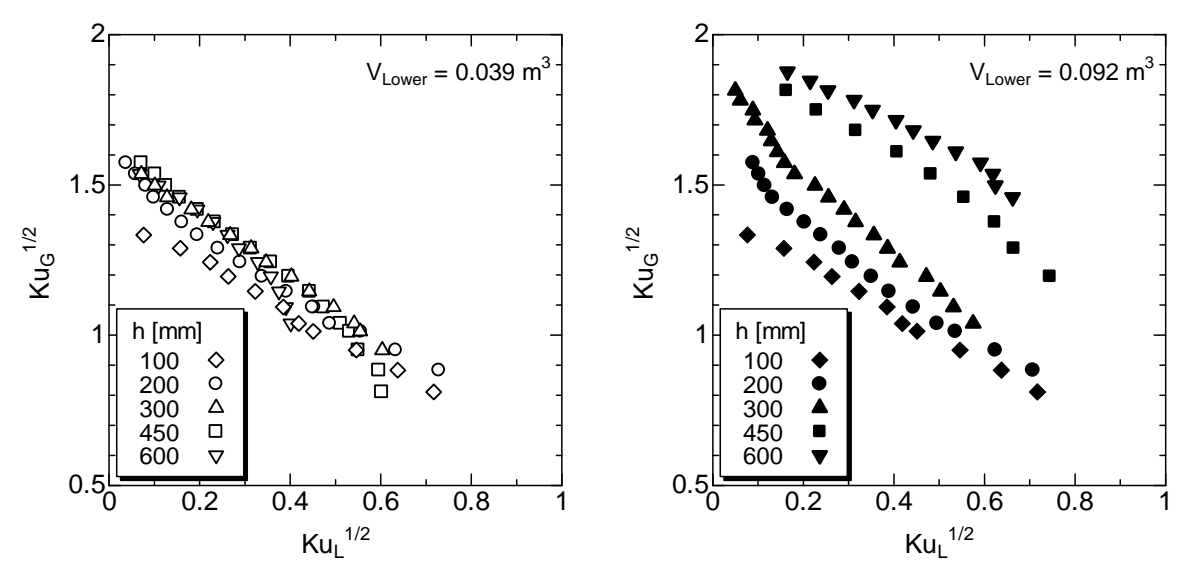


Figure 11 Effects of water level, h, in upper tank on CCFL characteristics (D = 30 mm)

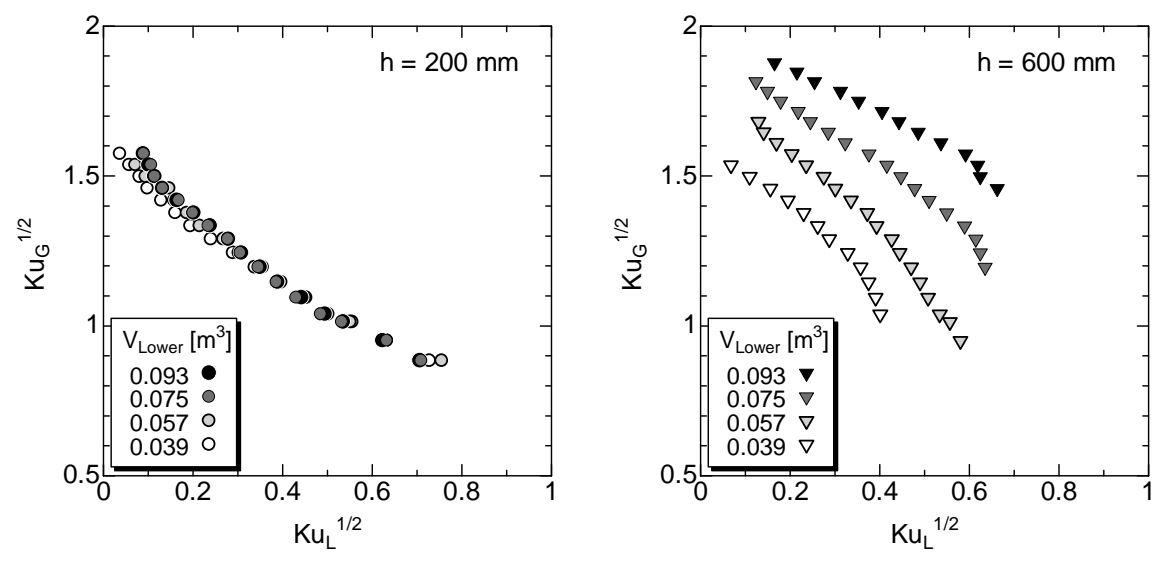


Figure 12 Effects of lower tank volume, V_{Lower} , occupied by air on CCFL characteristics (D = 30 mm)

Figure 13 shows the pressure differences for the cylindrical tank (b) and their power spectrums. The time-averaged ΔP increases with the water level in the upper tank, which corresponds to the water head in the upper tank. The amplitude of the pressure fluctuation at h=450 mm is larger than that at h=200 mm, and the fluctuation frequency at h=450 mm is lower than that at h=200 mm. Images of flow patterns in the middle part of the vertical pipe for h=450 mm and $V_{Lower}=0.039$ m³ are shown in Figure 14. The amount of falling liquid film is small at t=0.30 s. The large water lump falls for 0.32 < t < 0.34 s. The ΔP increases during the water lump falling. Then the liquid film flows back to the upper tank and the ΔP decreases. The liquid film restarts to fall at t=0.98 s. The amount of the falling water lump is small at low h and low V_{Lower} , and it becomes larger as h and V_{Lower} increase. This is the main cause of the difference in the CCFL characteristics for different values of h and V_{Lower} .

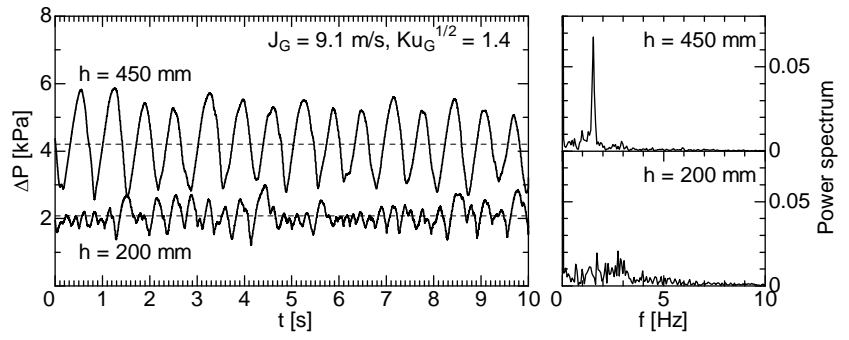


Figure 13 Pressure difference ΔP between upper and lower tanks (Cylindrical tank (b), D = 30 mm, $V_{Lower} = 0.092$ m³ and $J_G = 9.1$ m/s)

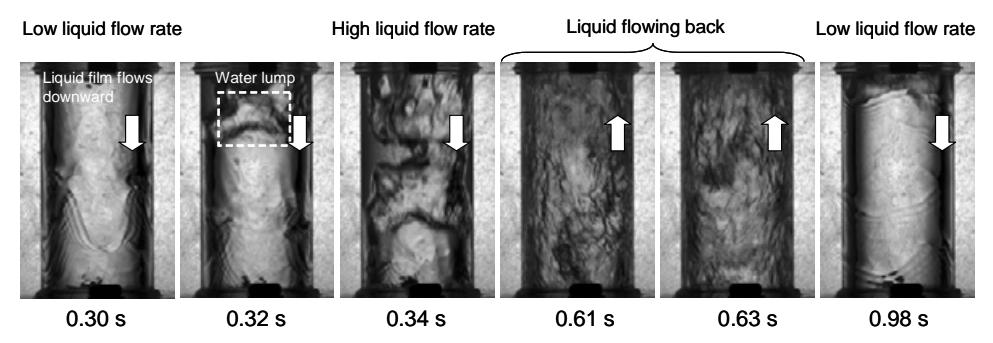


Figure 14 Flow patterns at the middle of the vertical pipe (Cylindrical tank (b), D = 30 mm, h = 450 mm, $V_{Lower} = 0.092$ m³ and $J_G = 9.1$ m/s)

4. Conclusion

Counter-current flow limitation (CCFL) in vertical pipes are measured using an apparatus consisting of the vertical pipe, the upper tank and the lower tank to understand effects of tank geometry and water level in the tanks. The tank geometries used were rectangular and cylindrical. The pipe diameters tested were 30, 45 and 60 mm. Air and water at room temperature and atmospheric pressure were supplied from the upper tank and from the lower tank, respectively. The flow rate of water entering into the lower tank was measured to obtain CCFL characteristics. Flow patterns in the upper tanks were observed by using a high-speed video camera and the pressure difference between the upper and lower tanks was measured to understand relations between CCFL characteristics and the flows in the tanks. The main conclusions obtained are as follows:

- (1) The CCFL characteristics for different pipe diameters are well correlated using the Kutateladze number if the tank geometry and the water levels in the tanks are the same.
- (2) CCFL takes place at the junction between the pipe and the upper tank both for the rectangular and cylindrical tanks. In addition, CCFL with the cylindrical tank (a) takes place not only at the junction but also inside the pipe when the gas flow rate is high and the pipe diameter is small.
- (3) CCFL at the junction of the rectangular tank is stronger than that at the junction of the cylindrical tank (a) because of the presence of low frequency first-mode sloshing in the rectangular tank.

(4) Water penetration into the pipe increases with the water level, h, in the cylindrical upper tank and the lower tank volume, V_{Lower} , occupied by the air, and therefore, the CCFL are to be mitigated with increasing h and V_{Lower} .

These experimental results clearly show that not only the pipe geometry but also tank geometry and water levels in the tanks must be taken into account when modelling characteristics of CCFL in vertical pipes.

References

- [1] C. Yanagi, T. Nariai, T. Futatsugi, A. Tomiyama, I. Kinoshita and M. Murase, Countercurrent Air-Water Tests Using a Scale Model of a Pressurizer SurgeLine, Proceedings of ICONE19-43222, 2011.
- [2] G. B. Wallis, A. S. Karlin, C. R. Clark, III, D. Bharathan, Y. Hagi and H. J. Richter, Countercurrent Gas-Liquid Flow in Parallel Vertical Tubes, Int. J. of Multiphase Flow, Vol. 7, pp. 1 19, 1981.
- [3] D. Bahrathan, G. B. Wallis and H. J. Richter, Air Water Countercurrent Annular Flow in Vertical Tubes, EPRI NP-786, May 1978.
- [4] C. L. Tien and C. P. Liu, survey on Vertical Two-Phase Countetcurrent Flooding, EPRI NP-984, Electric Power Research Institute, 1979.
- [5] D. J. Nicklin and J. F. Davidson, The Onset of Instability in Two-Phase Slug Flow, Proc. Symp. Two-Phase Fluid, No. 4, Institution of Mechanical Engineers, London, 1962.
- [6] H. J. Richter, Flooding in Tubes and Annuli, Int. J. Multiphase Flow, Vol. 7, 647-658, 1981.
- [7] C. P. Liu, C. L. Tien and G. E. McCarthy, Flooding in Vertical Gas-Liquid Countercurrent Flow through parallel Path, EPRI-NP-2262, 1982.
- [8] Y. Sudo and T. Usui and M. Kaminaga, Experimental Study of Falling Water Limitation under a Counter-Current Flow in a Vertical Rectangular Channel, JSME Int. J., Ser-II, 34-2, 169-174, 1991.
- [9] J. H. Jeong and H. C No, Experimental Study of the Effect of Pipe Length and Pipe End Geometry on Flooding, Int. J. Multiphase Flow Vol. 22, No. 3, 499-514, 1996.
- [10] F. Kaminaga, Y. Okamoto and Y. Shibata, Evaluation of Entrance Geometry Effect on Flooding, Proc. 1st JMSE/ASME Joint Int. Conf. on Nucl. Eng., Tokyo, 95, 1991.
- [11] G. B. Wallis, One-dimensional Two-phase Flow, McGraw Hill, p. 339, 1969.
- [12] S. S. Kutateladze, Elements of the Hydraulics of Gas-Liquid System, Fluid Mechanics Soviet Research, Vol. 1, No. 4, 1972, p. 29.
- [13] O. R. Jaiswal1, Shraddha Kulkarni and Pavan Pathak, A Study on Sloshing Frequencies of Fluid-Tank System, The 14th World Conf. on Earthquake Engineering October 12-17, 2008, Beijing, China.